Molecular Dynamics simulation of molecular crystals under anisotropic compression: bulk and directional effects in anthracene and paracetamol

Journal:	*Crystal Growth & Design*
Manuscript ID	cg-2020-01098a.R3
Manuscript Type:	Article
Date Submitted by the Author:	n/a
Complete List of Authors:	Rizzato, Silvia; Universita degli Studi di Milano, Dipartimento di Chimica Gavezzotti, Angelo; Universita degli Studi di Milano, Dipartimento di Chimica Lo Presti, Leonardo; Università degli Studi di Milano, Department of Chemistry

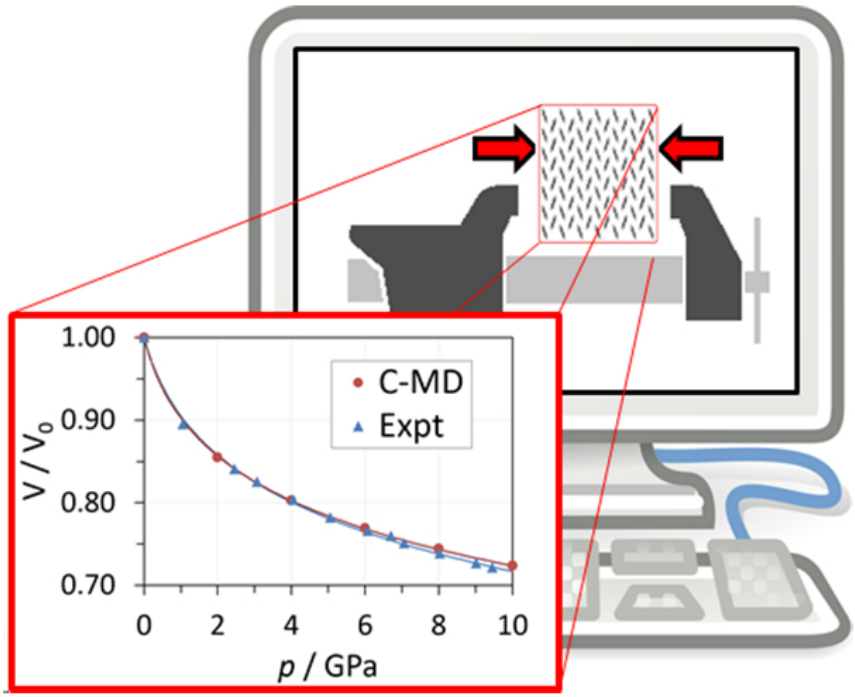

Table of content graphics: Computer simulation of molecular crystals by classical molecular dynamics under both isotropic and anisotropic external stress fields reproduces quantitatively the response of the material at high pressure, shedding light on the implied changes at the molecular–scale.

59x44mm (300 x 300 DPI)

Molecular Dynamics simulation of molecular crystals under anisotropic compression: bulk and directional effects in anthracene and paracetamol

Silvia Rizzato,[a] Angelo Gavezzotti,[a] Leonardo Lo Presti[a,*]

[a] Department of Chemistry, Università degli Studi di Milano, Via Golgi 19, 20133 Milano (Italy)

[*] To whom correspondence should be addressed: leonardo.lopresti@unimi.it

Abstract

The Parrinello-Rahman pressure-control algebra with anisotropic external stress field, , coupled with recently developed, accurate atom-atom potentials, has been incorporated in new modules of the Milano Chemistry Molecular Simulation (MiCMoS) computer program package for application in Molecular Dynamics simulations for organic crystals. Simulations were carried out for two widely different intermolecular environments, anthracene and paracetamol. The results reproduce quantitatively the anisotropic evolution obtained by pressure-dependent X-ray diffraction experiments in hydrostatic conditions. A less usual application concerns the probing of differently oriented uniaxial stress, which for anthracene reveal a phase transition triggered by mechanical excitation along a direction parallel to the main molecular axis. For paracetamol, differences in compressibility along different crystal directions are borne out and are explained in molecular terms with reference to the hydrogen bonding scheme. Simulations of tensile stress, that is, negative pressure along different crystal directions, provide an estimate of yield points in a range of 0.2-0.5 GPa (2000-5000 atmospheres) and indicate the weakest directions. On the basis of these results we strongly suggest that classical MD in the atom-atom formulation, even in absence of thorough treatment of quantum effects, but endowed with flexible algebra and coupled with carefully calibrated intermolecular potentials, can give reliable results of quantitative and semi-quantitative character on the structural dynamics of organic crystals, providing an essential support to downstream studies of mechanical, optical and electronic properties. Widespread use for further experience and validation is encouraged by the availability of the Fortran source codes.

Introduction

X-ray crystallography has given for half a century a fundamental contribution to quantitative understanding of molecular recognition and crystal packing. For all its merits, it does however provide only a space–time average picture, a limitation that obscures entropic and vibrational effects on cohesive energies.[1–3] Dynamic information from standard X-ray diffraction experiments is confined to atomic displacement parameters (ADPs), whose interpretation is not always immediate in terms of fundamental physics.[4,5] Accounting for dynamic effects is obviously desirable in principle and also for cutting-edge applications like, for example, energy transduction[6] and shape–changing materials.[7] Moreover, thermal expansion coefficient and isothermal compressibility rely on dynamic interplay among intermolecular interaction forces, often comprehensively dubbed non-covalent interactions (NCIs). Activation by external stimuli, such as changes in temperature and pressure, alter the whole dynamics, often allowing access to new equilibrium or metastable structures. Experimental high–pressure crystallography may in principle give quantitative estimates of elastic properties and offer help for a description of the response of NCIs, but it is fraught with numerous practical difficulties and its results may be sensitive to a number of boundary conditions.[8]

On the computational side, quantum simulations mostly provide a static and temperature-less picture, while accounting for finite temperature and pressure effects is computationally demanding;[9] dynamic simulation of organic crystals in the nanosecond range are definitely out of reach for state–of–art quantum methods. Classical molecular dynamics (C-MD) is much more affordable and can deal with computational boxes of hundreds or thousands of molecules and, at variance with simple minimization procedures, it can explicitly account for finite T and p effects. C-MD requires careful calibration of intermolecular potentials; besides, being an equipartition-regime technique, it suffers from the absence of quantum effects.[10,11] Its results are however quite trustable at or around room temperatures as demonstrated by a vast literature.[10,12–15] Its performance in high pressure or anisotropic environments need be carefully validated, and this will be one of the aims of the present paper.

In C-MD studies, temperature control is handled by a number of rather simple and reliable techniques, while pressure control is more problematic. An elegant and efficient algorithm has been developed by Parrinello & Rahman[16,17] originally applied to metallic systems; we present here an adaptation of PR for application of a generalized anisotropic pressure or stress field to molecular crystals. The existing literature on pressure-dependent

molecular simulation for organics is rather scanty[18–22]; and yet, pressure control can be important for practical applications of organic compounds. For testing and validation, among the few compounds for which experimental variable-*p* studies are available, we chose two crystalline materials with different properties and intermolecular recognition modes: anthracene[23], the parent of the polyacene family with pressure-dependent physical and optoelectronic properties, and the hydrogen-bond dependent structure of paracetamol,[24,25] which, like all APIs (Active Pharmaceutical Ingredients), is subject to pressure gradients during drug formulation. The algorithm is implemented in the Milano Chemistry Molecular Simulation (MiCMoS) package[26–28] and is available for public use. In general, the effect of pressure on unit cell parameters is of major importance in crystallography and materials science. To the best of our knowledge, no widespread software exists, which explicitly focuses on the simulation of small organic molecules in their condensed state, especially as a function of an external anisotropic stress field. MiCMoS was created to fill this gap: it can handle pure liquids, solutions, crystals and nanoclusters of small organics on a common PC environment, with a minimum intervention by the user. Most important, the package embeds two force fields, CLP and LJC, which rely on accurately calibrated intermolecular potentials able to reproduce quantitatively key thermodynamic quantities of the condensed state of several small organic compounds.[29]

Our goal here is to simulate the effect of increasing hydrostatic (isotropic) pressure in comparison with experiment; then, the response of each structure against anisotropic or uniaxial stress fields is also computed, including tensile (negative pressure) stress. The results are first validated by good agreement with experimental crystallographic data; then, it is shown that they shed light on the dynamic role of NCIs, on relative polymorph stabilities, and on probable mechanisms of pressure–induced crystal–to–crystal phase transitions. The whole computational setup shows good promise for probing a so far almost uncharted molecular simulation territory.

METHODS

Pressure control algorithm

The original algebra developed by PR[16,17] relies on Lagrangian dynamics applied to the 3x3 Cartesian cell edge tensor, **H**. The basic equations are:

$$\mathbf{F} = w\frac{d^2\mathbf{H}}{dt^2} = [\mathbf{P} - p\mathbf{I}]\boldsymbol{\sigma} - \mathbf{H}\cdot\boldsymbol{\Sigma} \qquad (1)$$

$$\boldsymbol{\Sigma} = \left[\mathbf{H_0^{-1}}(\mathbf{S} - p\mathbf{I})\tilde{\mathbf{H}}_\mathbf{0}^{-\mathbf{1}}\right] \cdot V_0 \quad (2)$$

F is the force acting on the simulation box tensor, **P** is the pressure tensor from the virial field, *p* is the scalar (target) hydrostatic pressure, **I** is the identity matrix and **σ** is the volume-scaled reciprocal cell matrix. *w* is a coupling parameter with dimensions of a mass, which determines the inertial response of the lattice to the pressure unbalance. $\mathbf{H_0}$ is the starting (undistorted) simulation box tensor. The external stress is added through a 2nd–order symmetric tensor, **S**; the symmetric tensor **Σ** converts the applied stress into a surface energy density by accounting for the shape of the unit cell. Eq. 1 complies with a standard leap–frog integrator; the velocity matrix $\mathbf{V_H}$ associated to cell edge under force **F** is estimated as

$$\mathbf{V_H} = \frac{1}{2}\left(\frac{n \cdot \Delta t}{w}\right)\mathbf{F} \quad (3)$$

where *n* is the number of MD steps between two anisotropic scaling procedures and Δ*t* is the simulation timestep. Finally, the Cartesian cell edge vectors **H** are updated:

$$\mathbf{H}(t + \Delta t) = \mathbf{H}(t) + (n \cdot \Delta t)\mathbf{V_H} \quad (4)$$

and all molecules in the simulation box are rigidly translated accordingly. A fully detailed description of the algorithm is in Section S1 of the Supplementary Information (SI).

MD simulations

The procedure has been applied to anthracene at room pressure[30] (CSD: ANTCEN), then to high–*p* data up to 10 GPa available from an X–ray powder diffraction (XRPD) study;[23] and to monoclinic ($P2_1/n$) and orthorhombic (*Pbca*) polymorphs of paracetamol[31,32] (CSD: HXACAN27 and HXACAN33). For the monoclinic form, single crystal X-ray data are available up to 4 GPa,[24] while the orthorhombic form underwent only XRPD experiments at high *p*.[25]

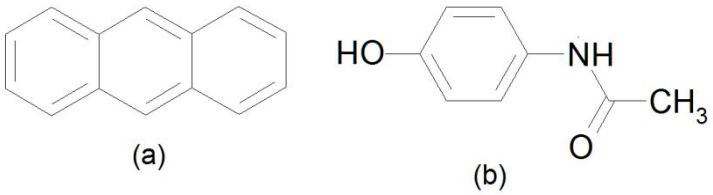

Scheme 1. Molecular structures of anthracene (a) and *N*-(4-hydroxyphenyl)acetamide (paracetamol) (b).

The force fields selected[29] were the Coulomb-London-Pauli (CLP) for anthracene and the Lennard-Jones-Coulomb (LJC) one for paracetamol (justification in Section S1.2.1 of SI). These are atom-atom force fields carefully and extensively calibrated on structural and

thermochemical properties of hundreds of organic crystals. Computational boxes with sides of ~30–40 Å were built through replicas of the unit cell. Isothermal–isobaric (*NpT*) simulations were carried out at timesteps of either 1 or 2 fs. First, each crystal was equilibrated for 1 ns at $T = 300$ K and $p = 1$ atm, with no external stress field **S**. Temperature was controlled by a Berendsen-type weak coupling (justification in Section S1.2.2 of SI). After preliminary ambient equilibration with coupling parameter $w = 3$ kg, isotropic stress fields **S** were applied with an optimized $w = 10$ kg and $p = 0$ (see PR[17] and Section S1 of SI) for 1 ns as well. Anisotropic stress fields were then applied along the Cartesian reference directions (see Section S1 SI), roughly parallel to crystallographic cell edges, for 200 ps. From the trajectories, mean crystallographic structures were obtained by time–averaging atomic coordinates over the last 50 or 100 frames and then by space–averaging over the translational replicas; average structures were represented with all molecules in the unit cell symmetry-independent, in a formally *P*1 space group. A complete list of topologies for MD simulations, including force field parameters and input files, is available in Section S2 SI.

Results and discussion

Anthracene

Anthracene crystallizes in space group $P2_1/a$, adopting the herringbone motif typical of linear conjugated aromatics with an angle of ~50° between molecular planes. Polyacenes are molecular materials for organic electro–optical devices, with absorption and luminescence responses coupled with large carrier mobility due to the tuneable overlap of extended aromatic π systems.[33] These properties depend on the arrangement of planar cores, obviously sensitive to applied pressure.

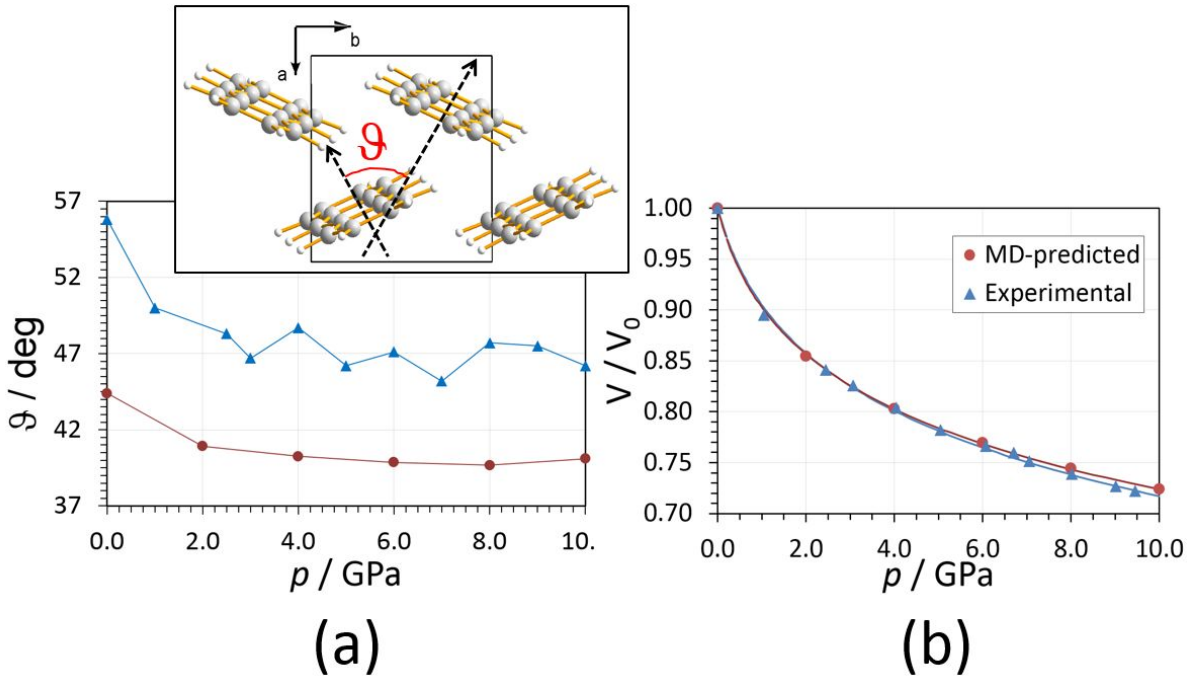

Figure 1. (a) Predicted (red dots, this work) *vs*. experimental (blue triangles)[23,34] interplanar angle ϑ as a function of pressure. Inset: definition of the angle ϑ. Lines serve only as a guide for the eye. (b) Predicted (red dots, this work) *vs*. experimental (blue triangles) relative change of the anthracene cell volume up to 10 GPa. V_0 corresponds to ambient conditions. Lines are the least-squares fittings based on the Vinet equation of state.[35] Individual cell edges are reported in Figure S3 SI.

Figure 1 shows the results of C-MD simulations at isotropic pressure between ambient and 10 GPa. The changes in lattice parameters and cell volume between 1 atm and 10 GPa are reproduced quantitatively (see Table S1 SI and Figure S3 SI). The ϑ angle (Figure 1a) is slightly underestimated at ambient pressure, in a well-known shortcoming of atom-atom treatments that prefer flatter stacking; it decreases by ≈ 4 deg (–9 %, from 44.4 to 40.2 deg) at 4 GPa and then stays essentially constant, in good agreement with the experimental trend, where the change is from 55.8 to 46.2 deg (–8 %).[23] Fitting of volume data (Figure 1b) gives estimates for the isothermal bulk modulus and its first derivative at zero pressure, B_0 = 5.55(1) GPa and B_0' = 11(3) in close agreement with experiment, B_0 = 6.1(2) GPa and B_0' = 9.8(3). Center-of-mass radial distribution functions (Figures S4 and S5 SI) show the expected contraction of intermolecular distances with increasing pressure.

Conflicting evidences exist on the occurrence of a high–pressure structural phase transitions of anthracene.[23,36,37] The final line seems to be that no phase transition exists, and traces of transition were ascribed instead to imperfect control of hydrostatic conditions.[8] In our simulations, an increment of external pressure to 30 GPa produces a minor loss of symmetry in the first coordination shell (Figures S6 and S7 SI), but the structure remains

fully compatible with that at ambient conditions. In conclusion, no phase transitions are detected if the applied stress is perfectly hydrostatic , in agreement with experimental findings.[8]

The picture changes drastically when even a relatively moderate compression is applied anisotropically along one laboratory axis. Figure S8 (SI) shows the results for a 0.5 GPa compression along X and Y Cartesian axes. Distortion of cell shape and rearrangements of interplanar structure occur but once again there is no change in overall crystal symmetry. Especially noteworthy is the result of compression along Z, that is, roughly parallel to *c* (Figure 2): this does not dramatically alter the centre of mass distances in the first coordination shell (Figure S8b SI), but causes the monoclinic angle to increase by ≈ 12° and eventually breaks the glide symmetry in the (*a*,*b*) plane.

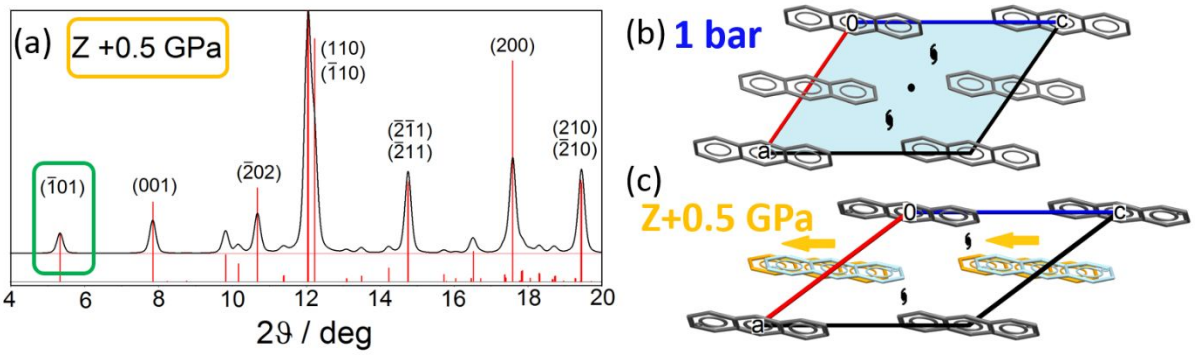

Figure 2. (a) Simulated powder pattern (same parameters as in Figure S7 SI) for anthracene averaged over the last 100 ps of a 200 ps–long trajectory under uniaxial compression of 0.5 GPa along the laboratory axis Z. The $(\bar{1}01)$ reflection, symmetry–forbidden in $P2_1/a$, is highlighted in green. (b) Crystal packing of anthracene at ambient pressure in the (*a*,*c*) plane, with highlighted the *a* glide (cyan), the screw axes and the inversion centre. (c) Anthracene under uniaxial compression, viewed down the *b* axis. Molecules at ½ *a* corresponding to the actual C–MD prediction are coloured in yellow; cyan ones indicate where they would be if the glide *a* were still present. The yellow arrows highlight the slip direction.

The reason is that rows of molecules packed along *a* slip back by roughly 1/6 of the main molecular axis with respect to each other (Figure 2c), destroying the inner translational component (½**a**) of the glide. Therefore, a low–angle $(\bar{1}01)$ reflection appears (Figure 2a), which would be extinct in $P2_1/a$ while it is fully compatible with the same signal found experimentally above 10 GPa.[8] Symmetry checks[38] hint at a reduction of space group to $P2_1$ for the final frames of our simulation (Section S3.1 SI). We thus predict the existence of a polar high–*p* structure of anthracene, which might happen also in isostructural higher polyacenes, and could open new perspectives for the use of anisotropic stress fields to

develop unexpected response properties even in simple materials. This prediction awaits further experimental testing. While we cannot claim to have scanned most or the whole of anthracene crystal phase space at high pressure, a pressure-induced (not "spontaneous") transition is neatly detected, in agreement with present experimental findings. In any case, the result is confirmed even when the simulation under compressive uniaxial stress is extended to 1 ns (see Figure S8d,e SI).

Paracetamol

Paracetamol is a well known analgesic and antipyretic compound and its solid-state phase behaviour, comprising at least six polymorphs, has been extensively studied: a summary of the current knowledge is presented in Section S4.1 of SI. Our simulations are restricted to the monoclinic (henceforth B1) and orthorhombic (henceforth B2) phases,[39] the only ones for which diffraction data at 1, 2, 3 and 4 GPa are available,[24,25] with full structure data for monoclinic and cell data only for orthorhombic.

The molecular conformation, as estimated by X–ray crystallography is nearly identical in the two phases (Figure S9 SI), but for a very minor difference in the angle χ between ring and amide planes (23-18°). The corresponding C–MD estimates at ambient T and p are 22 and 13º, in quantitative agreement with experiments. Packing diagrams are shown in Figure 3: in both structures, chains of O···H-O alcohol hydrogen bond are formed, linked by a zip of transverse N-H···O hydrogen bonds. However, monoclinic B1 shows strongly corrugated sheets, with a large angle between successive aromatic planes; in the orthorhombic B2 structure, the layers are much less corrugated, actually not far from planar, this being presumably the reason for the better tabletting properties[40] of this polymorph.

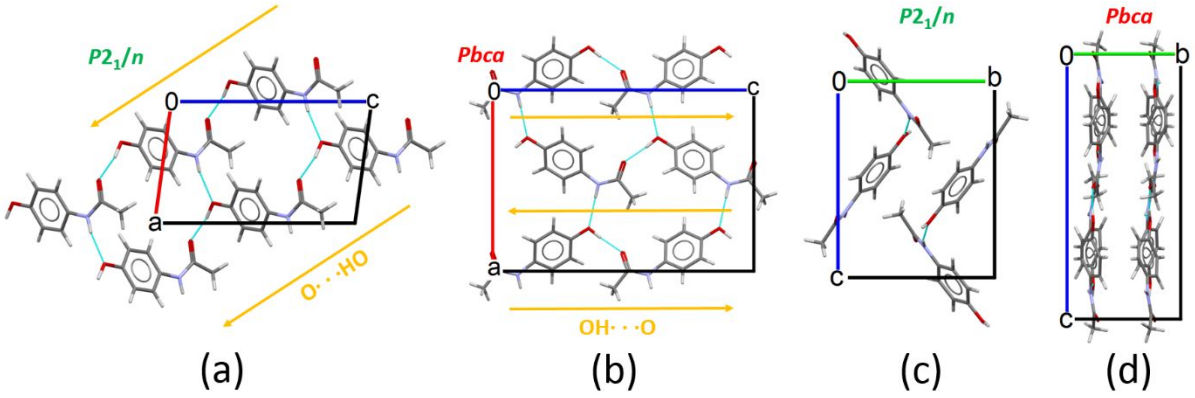

Figure 3. Paracetamol packing as seen down the *b* axis ((a) monoclinic, (b) orthorhombic) and the *a* axis ((c) monoclinic, (d) orthorhombic). H-bonds are drawn as cyan dotted lines. Yellow arrows highlight the direction of OH···O bonds; N-H···O links are orthogonal.

Figure 4 and Table 1 show the relative changes of lattice parameters of both polymorphs as a function of pressure. Both experiments and C–MD simulations agree in estimating identical bulk moduli B for the two phases, even though the theoretical predictions are systematically smaller (Figure 4a). Least squares fitting with the Vinet equation of state hints B = 6.23(3) (C–MD) or 9.64(3) GPa (experimental) for the $P2_1/n$ phase, and B = 6.62(3) GPa (C–MD) or 9.29(4) GPa (experimental) for the *Pbca* one. In any case, the absolute agreement among lattice parameters and cell volume changes is good (Tables S2 and S3 SI), becoming quantitative when relative changes of crystallographic parameters are considered (Table 1).

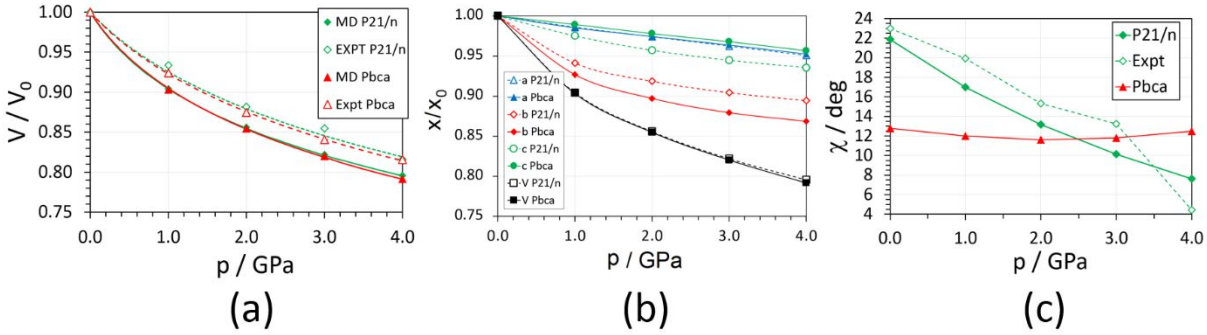

Figure 4. (a) Relative change of the cell volume of paracetamol, from either X-ray diffraction estimates (empty dots, dashed lines)[24] and C–MD simulations (full dots, full lines). Lines are the least-squares fittings based on the Vinet equation of state.[35] (b) Comparison of relative changes of lattice parameters with isotropic pressure for the $P2_1/n$ (empty points) and *Pbca* (full points) structures, with the following colour code: blue: *a*; red: *b*; green: *c*; black: *V*. (c) Change of angle χ as a function of *p*. Full rhombi: C–MD simulations; empty rhombi: experimental,[24] both for the $P2_1/n$ structure. Red triangles: C–MD simulations, *Pbca* structure.

Table 1. Relative changes of cell parameters in paracetamol by MD simulations with LJC potentials, under isotropic PR pressure control, compared with experimental results upon going from 1 atm to 4 GPa.

	$P2_1/n$		*Pbca*	
Lattice parameter	Experimental	MD	Experimental	MD
a	–0.06	–0.05	–0.03	–0.04
b	–0.14	–0.11	–0.14	–0.12
c	+0.02	–0.06	–0.03	–0.03
β	+0.02	0.00	-	-

In the monoclinic polymorph, the *c* cell edge goes apparently through a minimum at *p* = 2 GPa and then increases, resulting in an overall +2% expansion at 4 GPa (Table 1). Rather, C–MD predicts a uniform decrease. The discrepancy is however very small and could result

either from minor failure of the force field or, more likely, by some hardly predictable experimental condition related to anisotropy in crystal shape or in compression medium.

Both structures are scarcely compressible along the *a* and *c* directions (Figure 4b), and much more compressible along the direction perpendicular to the layers, roughly parallel to *b* (Figure 3). In that direction, molecules can be brought closer without strong repulsion, accounting for the reduction of average molecular centre of mass distances (Figure S10 SI). On the contrary, the strong HB network in the (*a*,*c*) plane opposes the compression; for example, $\langle R(\mathrm{OH}\cdots\mathrm{O})\rangle$ decreases by just 0.1 Å at 4 GPa in both polymorphs (Figure S11, SI). Increasing pressure affects molecular conformation in widely different ways: in *Pbca*, the χ dihedral does not depend on *p*, while it flattens by as much as 14° in $P2_1/n$, forcing paracetamol in an almost planar conformation (Figure 4c). The same conformational change was reported experimentally.[24] The reason can be traced back in the different mutual orientation of the hydrogen bonded molecules (Figure 3c). Approaching of nearly parallel layers in *Pbca* along the most compressible direction *b* occurs just by reducing the distance among the sheets, without perturbing the HB pattern parallel to (*a*,*c*). On the contrary, the same contraction in the $P2_1/n$ lattice would distort OH···O contacts (Figure 3c). A small rotation of the amide group allows keeping favourable HB geometries within each sheet, contributing to alleviate the lattice strain.

Compression energetics

The total intermolecular energy of all crystal structures here considered become less stabilizing with increasing pressure as expected (Figure 5; see also Figures S12–S13 SI). Since the interaction functions were optimized using reference data at room conditions, it is reassuring to verify that the response of the potentials with pressure is reasonable. The rise in energy is due to a sharply increasing repulsion energy, while Coulombic terms become more stabilizing with decreasing distance (as is obvious from their functional form), but to a minor extent. Although quantitative estimates are problematic, and there is no way to check the predictions in against experiment, it is observed that the two curves for *E*(inter) cross at $p \approx$ 4.3 GPa, where the orthorhombic form becomes marginally more stable, at least in terms of intermolecular energy. This can again be traced back to the supposed higher compressibility of the layered orthorhombic phase. Decomposition of total intermolecular energy into Coulombic and dispersive–repulsive terms (Figure S12 SI) provides a possible molecular–basis explanation: the layered packing in *Pbca* (Figure 3c) favours attractive stacking

interactions, which make the increment of the repulsive energy less steep than in $P2_1/n$. Experiments on powdered monoclinic structure by B2[25] showed that an incomplete conversion of $P2_1/n$ into *Pbca* is possible at high *p*. However, as this transition is only observed after raising *p* to 4.2 GPa and then lowering it again down to 1.3 GPa, kinetics is expected to play a fundamental role in the process. We suspect that strain–induced defects created by the compression–decompression cycle, could help to lower the activation energy of the monoclinic → orthorhombic transition.

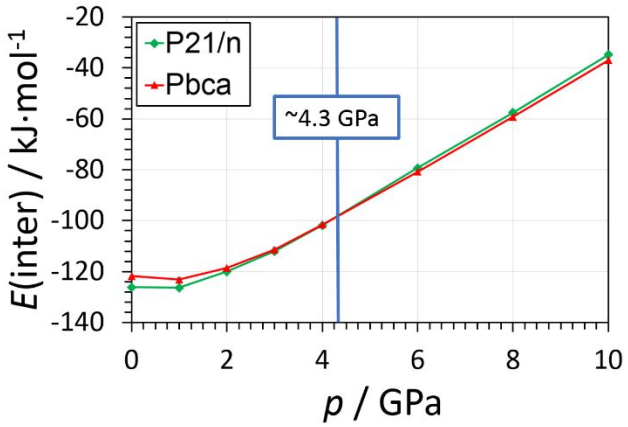

Figure 5. Intermolecular energy curves as a function of pressure for the two polymorphs of paracetamol. The vertical line marks the crossing point. Broken lines serve only as guides for the eye.

Tensile stress

Anisotropic hardness can reveal preferential orientation of possible cleavage planes and identify active slip systems able to accommodate the motion of dislocations during compression, and indeed such studies are applied to drugs, including paracetamol, since long time. Computational evidences can be extremely useful to complement and understand experimental outcomes[41]. Taking advantage of the newly introduced features for pressure control, anthracene and paracetamol were simulated also with *negative* pressures, implying a tensile stress, by 200 ps of *NpT* runs in the range ± 1 GPa (Figures 6 and S14–S15 SI). The crystals do not survive a tensile stress higher than 0.2 -0.5 GPa; this result, not unexpected in molecular compounds characterized by soft NCIs, is anyway a genuine prediction of a property that cannot be easily investigated experimentally. Some representative examples of crystals breaking apart after excessive cell volume increase are deposited as mp4 video files as SI.

The lattice undergoes larger tensile deformations along directions where strong NCIs cannot be set up, such as Z (roughly parallel to *c*, perpendicular to (001) planes in anthracene and Y (parallel to *b*, perpendicular to (010) planes in paracetamol. In anthracene, CH···π

interactions are directed roughly along the (*a*,*b*) diagonal, corresponding to the [110] direction, and in fact X and Y are the less deformable directions. Paracetamol breaks preferentially along Y ([010]), (the softest stacking direction), while strong HB in the (*a*,*c*) plane oppose tensile deformation along [100] and [001]. A monoaxial compression causes instead the corresponding cell edge to shorten (Figures S13 and S14 SI), but the length of the other two cell edges increases, minimizing as much as possible the overall change in volume (Figures 6). This seems to be a general rule, at least for the systems here studied. When compression is applied along the soft direction of paracetamol ([010] or Y), *a* and *c* still increase (Figure S14 SI), but the overwhelming shortening of *b* allows a significant reduction of the volume (Figure 6b,c).

In our opinion, the main take–home message is that great care should be taken to interpret outcomes from high–pressure crystallography experiments, as imperfect isotropic compression might easily result in uneven changes of lattice parameters. Simulating uniaxial compression by C–MD can help to disentangle the physics behind unexpected or odd experimental outcomes.

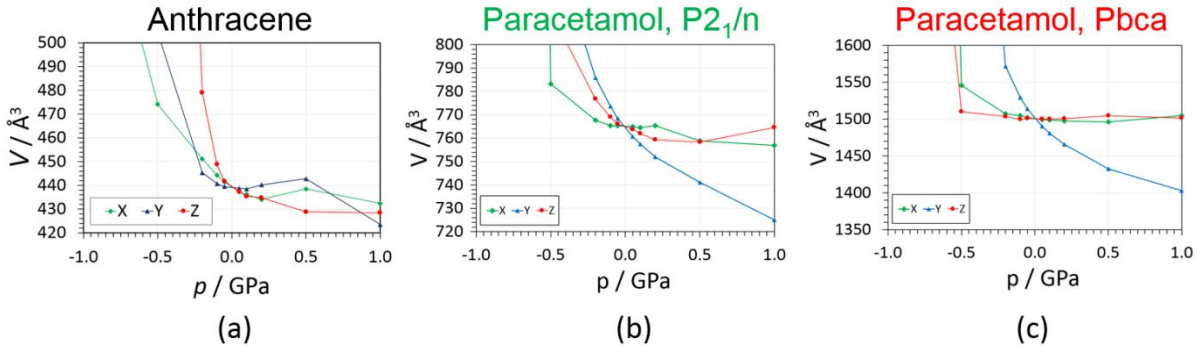

Figure 6. (a) Change of the cell volume due to a monoaxial stress field applied along either the X (green), Y (blue) or Z (red) laboratory axis (V, Å^3) of anthracene. Negative (positive) p means tensile (compression) stress. All data points come from the average of the last 100 ps of 200 ps–long NpT trajectories. For each simulation, $S_{ij} = 0$; two diagonal elements of **S** were set at $1.033 \cdot 10^{-4}$ GPa, while the third one followed the sequence –1, –0.5, –0.2, –0.1, –0.05, +0.05, +0.1, +0.2, +0.5, +1.0 GPa. (b) and (c): Same as (a), for the two $P2_1/n$ and *Pbca* forms of paracetamol.

Summary and Conclusions

An adaptation of the Parrinello-Rahman pressure-control algebra, coupled with recently developed, accurate atom-atom potentials, has been incorporated in new modules of the Milano Chemistry Molecular Simulation (MiCMoS)[28] computer program package for

application in Molecular Dynamics simulations for organic crystals. Simulations of anisotropic evolution under uniform pressure for two widely different intermolecular environments, anthracene and paracetamol, reproduce quantitatively the results obtained by pressure-dependent X-ray diffraction experiments in hydrostatic conditions, thus confirming the adequacy of the potentials and the applicability of the algorithm.

The procedure allows the application of a user-specified external stress tensor, giving access to fine detail of crystal anisotropy. For anthracene, the analysis of differently oriented uniaxial stress reveals a phase transition triggered by mechanical excitation along a direction parallel to molecular axis, with a shear displacement that reduces crystal symmetry from $P2_1/a$ to $P2_1$; while the predicted transition has some features in common with experimental evidence, more experimental work is needed for further confirmation along our suggestion. For sure, anisotropic effects are largely dependent on the experimental conditions, including not only imperfect hydrostaticity of the pressure–transmitting medium, but also size, shape and quality of the crystals.

Two of the many polymorphs of paracetamol were simulated and the results were compared with evidence provided by variable-*p* X-ray diffraction experiments. Intermolecular energy curves as a function of pressure cross at 4.3 GPa, providing at least a hint at the existence of a controversial monoclinic-orthorhombic phase transition. The differences in compressibility along different crystal directions are borne out by our simulations and are explained in molecular terms by differences in resilience along a direction perpendicular to layers formed by hydrogen-bonded chains. A subtle effect, the negative compressibility along the *c* crystal axis of the monoclinic polymorph, could be analysed by a detailed analysis of uniaxial stress components.

Simulations of tensile stress, that is, negative pressure along different crystal directions, is also possible in our newly developed setup. The yield points of course vary with different strength of the anisotropic crystal adhesion; our simulations suggest a range of 0.2-0.5 GPa (2000-5000 atmospheres) and indicate the weakest directions, providing a genuine prediction of a property whose experimental probing is awkward.

In general, MiCMoS should be taken as a help alongside the exploration of experimental findings. Indeed, it relies on simple and fast procedures that necessarily require some approximations. For example, the implementation of thermostats more accurate than simple isokinetic velocity rescaling algorithms, like the Bussi-Donadio-Parrinello one,[42] is in order in future versions of the code. The purpose is to generate a correct microcanonical ensemble to deal with small clusters and nucleation problems, where correct sampling of low-

energy degrees of freedom is of utmost importance. We do not expect to stand up against more refined and widely used MD packages, but the results are promising and we believe that the code might be very useful in practical crystallographic applications. We strongly suggest that classical MD in the atom-atom formulation, even in absence of thorough treatment of quantum effects, when endowed with flexible algebra and coupled with carefully calibrated intermolecular potentials, can give reliable results of quantitative and semi-quantitative character on the structural dynamics of organic crystals, providing an essential support to downstream studies of mechanical, optical and electronic properties. This is particularly interesting in light of the relative ease to use of the free MiCMoS package, which is specifically oriented toward crystallographic problems with minimal requests for user intervention. Moreover, the results demonstrate once again that CLP and LJC are suitable force field schemes for use in organic crystal chemistry, with a majority of benefits over a minority of shortcomings, as seen in a previous work.[29] The agreement with experiment and other MD engines[27] is generally satisfactory, in the sense that the choice of a set of conditions primarily justifies itself by the results it obtains. An extensive comparison with other methods and other force fields will be possibly the topic of future studies. Widespread use for further experience and validation is encouraged by the (marginally conditional) availability of the source codes. Computational crystal chemistry for organic crystals seems to have come a long way from the early derivation of tentative functions for the estimate of simple lattice energies in the 1970s, to an evaluation of fine detail of anisotropic dynamics in these materials.

Acknowledgements

The Department of Chemistry at Università degli Studi di Milano is gratefully aknowledge for partial funding through the Development Plan for Atheneum initiative – Line B (Piano di Sviluppo dell'Ateneo – Linea B).

Conflict of interest

The Authors declare no competing conflict of interest

Supporting Information is available

Detailed description of the pressure control algorithm. Justification for the choice of force fields and thermostats. Equivalence of different p settings in the algorithm. Input topologies. Input files for molecular dynamics. Phase behaviour of polyacenes. Results for anthracene.

Average structure of anthracene under uniaxial compression (0.5 GPa). Platon ADDSYM output. Phase behaviour of paracetamol. Results for paracetamol. Cohesive energies (hydrostatic). Results in anisotropic (uniaxial) stress field. Animations of representative trajectories discussed in this work. This material is available free of charge via the Internet at http://pubs.acs.org.

Corresponding author

* Leonardo Lo Presti, Department of Chemistry, Università degli Studi di Milano, Via Golgi 19, 20133 Milano (Italy), Phone: +390250314252, Fax: +390250314300, e-mail: leonardo.lopresti@unimi.it

Author contributions

Algorithm development: LLP. MiCMoS development: AG, LLP. Investigation: LLP, SR. Writing: LLP, AG and SR. All authors have given approval to the final version of the manuscript.

REFERENCES

(1) Nyman, J.; Day, G. M. Modelling Temperature-Dependent Properties of Polymorphic Organic Molecular Crystals. *Phys. Chem. Chem. Phys.* **2016**, *18*, 31132–31143.

(2) Engkvist, O.; Price, S. L.; Stone, A. J. Developments in Computational Studies of Crystallization and Morphology Applied to Urea. *Phys. Chem. Chem. Phys.* **2000**, *2*, 3017–3027.

(3) Heit, Y. N.; Beran, G. J. O. How Important Is Thermal Expansion for Predicting Molecular Crystal Structures and Thermochemistry at Finite Temperatures? *Acta Crystallogr. Sect. B Struct. Sci. Cryst. Eng. Mater.* **2016**, *72*, 514–529.

(4) Finocchio, G.; Rizzato, S.; Macetti, G.; Tusha, G.; Lo Presti, L. Unravelling the Chemistry of the $[Cu(4,7\text{-Dichloroquinoline})_2Br_2]_2$ Dimeric Complex through Structural Analysis: A Borderline Ligand Field Case. *Crystals* **2020**, *10*, 477.

(5) Destro, R.; Lo Presti, L.; Soave, R.; Goeta, A. E. Multi-Temperature Electron Density Studies. In *Modern Charge-Density Analysis*; Gatti, C., Macchi, P., Eds.; Springer Netherlands: Dordrecht, 2011; pp 659–696.

(6) Lu, C.; Yang, Y.; Wang, J.; Fu, R.; Zhao, X.; Zhao, L.; Ming, Y.; Hu, Y.; Lin, H.; Tao, X.; et al. High-Performance Graphdiyne-Based Electrochemical Actuators. *Nat. Commun.* **2018**, *9*, 752.

(7) Papadopoulou, A.; Laucks, J.; Tibbits, S. Auxetic Materials in Design and Architecture. *Nat. Rev. Mater.* **2017**, *2*, 17078.

(8) Resel, R.; Oehzelt, M.; Shimizu, K.; Nakayama, A.; Takemura, K. On the Phase-Transition in Anthracene Induced by High Pressure. *Solid State Commun.* **2004**, *129*, 103–106.

(9) Parlinski, K. First-Principle Lattice Dynamics and Thermodynamics of Crystals. *J. Phys. Conf. Ser.* **2007**, *92*, 012009.

(10) Nemkevich, A.; Bürgi, H.-B.; Spackman, M. A.; Corry, B. Molecular Dynamics Simulations of Structure and Dynamics of Organic Molecular Crystals. *Phys. Chem. Chem. Phys.* **2010**, *12*, 14916.

(11) Dunitz, J. D.; Ibberson, R. M. Is Deuterium Always Smaller than Protium? *Angew. Chemie Int. Ed.* **2008**, *47*, 4208–4210.

(12) Wall, M. E.; Calabró, G.; Bayly, C. I.; Mobley, D. L.; Warren, G. L. Biomolecular Solvation Structure Revealed by Molecular Dynamics Simulations. *J. Am. Chem. Soc.* **2019**, *141*, 4711–4720.

(13) Ikeda, T. First Principles Isothermal-Isobaric Centroid Molecular Dynamics

Simulation of High Pressure Ices. *Chem. Phys. Lett.* **2019**, *717*, 141–146.

(14) Moncayo-Riascos, I.; Franco, C. A.; Cortés, F. B. Dynamic Molecular Modeling and Experimental Approach of Fluorocarbon Surfactant-Functionalized SiO_2 Nanoparticles for Gas-Wettability Alteration on Sandstones. *J. Chem. Eng. Data* **2019**, *64*, 1860–1872.

(15) van de Streek, J.; Alig, E.; Parsons, S.; Vella-Zarb, L. A Jumping Crystal Predicted with Molecular Dynamics and Analysed with TLS Refinement against Powder Diffraction Data. *IUCrJ* **2019**, *6*, 136–144.

(16) Parrinello, M.; Rahman, A. Crystal Structure and Pair Potentials: A Molecular-Dynamics Study. *Phys. Rev. Lett.* **1980**, *45*, 1196–1199.

(17) Parrinello, M.; Rahman, A. Polymorphic Transitions in Single Crystals: A New Molecular Dynamics Method. *J. Appl. Phys.* **1981**, *52*, 7182–7190.

(18) Rerat, B.; Rerat, C. Reconstitution Théorique de La Structure Cristalline de Composés Organiques Par Analyse Des Interactions Moléculaires En Dynamique Classique. Application Au Benzène Monoclinique Sous Haute Pression (Benzène III). *J. Chim. Phys.* **1990**, *87*, 2003–2015.

(19) Baidakov, V. G.; Tipeev, A. O.; Bobrov, K. S.; Ionov, G. V. Crystal Nucleation Rate Isotherms in Lennard-Jones Liquids. *J. Chem. Phys.* **2010**, *132*, 234505.

(20) Kohno, Y.; Mori, K.; Hiyoshi, R. I.; Takahashi, O.; Ueda, K. Molecular Dynamics and First-Principles Studies of Structural Change in 1,3,5-Triamino-2,4,6-Trinitrobenzene (TATB) in Crystalline State under High Pressure: Comparison of Hydrogen Bond Systems of TATB versus 1,3-Diamino-2,4,6-Trinitrobenzene (DATB). *Chem. Phys.* **2016**, *472*, 163–172.

(21) Kroonblawd, M. P.; Sewell, T. D. Predicted Anisotropic Thermal Conductivity for Crystalline 1,3,5-Triamino-2,4,6-trinitobenzene (TATB): Temperature and Pressure Dependence and Sensitivity to Intramolecular Force Field Terms. *Propellants, Explos. Pyrotech.* **2016**, *41*, 502–513.

(22) Galván, C. G.; Cabrera-Trujillo, J. M.; Hernández-Hernández, I. J.; Pérez, L. A. Molecular Dynamics Approach for Crystal Structures of Methane A and B. *Int. J. Mod. Phys. C* **2017**, *28*, 1750048.

(23) Oehzelt, M.; Resel, R.; Nakayama, A. High-Pressure Structural Properties of Anthracene up to 10 GPa. *Phys. Rev. B* **2002**, *66*, 174104.

(24) Boldyreva, E. V.; Shakhtshneider, T. P.; Vasilchenko, M. A.; Ahsbahs, H.; Uchtmann, H. Anisotropic Crystal Structure Distortion of the Monoclinic Polymorph of

Acetaminophen at High Hydrostatic Pressures. *Acta Crystallogr. Sect. B Struct. Sci.* **2000**, *56*, 299–309.

(25) Boldyreva, E. V; Shakhtshneider, T. P.; Ahsbahs, H.; Sowa, H.; Uchtmann, H. Effect of High Pressure on the Polymorphs of Paracetamol. *J. Therm. Anal. Calorim.* **2002**, *68*, 437.

(26) Gavezzotti, A.; Lo Presti, L. Dynamic Simulation of Liquid Molecular Nanoclusters: Structure, Stability and Quantification of Internal (Pseudo)Symmetries. *New J. Chem.* **2019**, *43*, 2077–2084.

(27) Gavezzotti, A.; Lo Presti, L. Molecular Dynamics Simulation of Organic Crystals: Introducing the CLP-Dyncry Environment. *J. Appl. Crystallogr.* **2019**, *52*, 1253–1263.

(28) Gavezzotti, A.; Lo Presti, L. MiCMoS - Milano Chemistry Molecular Simulation. MiCMoS User's Manual v1.1, 2020. See https://sites.unimi.it/xtal_chem_group. Milano.

(29) Gavezzotti, A.; Lo Presti, L.; Rizzato, S. Mining the Cambridge Database for Theoretical Chemistry. Mi-LJC: A New Set of Lennard-Jones–Coulomb Atom–Atom Potentials for the Computer Simulation of Organic Condensed Matter. *CrystEngComm* **2020**. Advance article.

(30) Mason, R. The Crystallography of Anthracene at 95°K and 290°K. *Acta Crystallogr.* **1964**, *17*, 547–555.

(31) Bouhmaida, N.; Bonhomme, F.; Guillot, B.; Jelsch, C.; Ghermani, N. E. Charge Density and Electrostatic Potential Analyses in Paracetamol. *Acta Crystallogr. Sect. B Struct. Sci.* **2009**, *65*, 363–374.

(32) Chan, E. J.; Goossens, D. J. Study of the Single-Crystal X-Ray Diffuse Scattering in Paracetamol Polymorphs. *Acta Crystallogr. Sect. B Struct. Sci.* **2012**, *68*, 80–88.

(33) Brütting, W. *Physics of Organic Semiconductors*; Brütting, W., Ed.; Wiley-VCH Verlag GmbH & Co. KGaA, 2005.

(34) Julian, M. M. *Foundations of Crystallography with Computer Applications*, 2nd ed.; CRC Press: Boca Raton,London,New York, 2014.

(35) Vinet, P.; Smith, J. R.; Ferrante, J.; Rose, J. H. Temperature Effects on the Universal Equation of State of Solids. *Phys. Rev. B* **1987**, *35*, 1945–1953.

(36) Zhao, L.; Baer, B. J.; Chronister, E. L. High-Pressure Raman Study of Anthracene. *J. Phys. Chem. A* **1999**, *103*, 1728–1733.

(37) Pufall, R.; Kalus, J. X-Ray Powder Diffraction of Anthracene at Hydrostatic Pressures up to 0.9 GPa. *Acta Crystallogr. Sect. A* **1988**, *44*, 1059–1065.

(38) Spek, A. L. Structure Validation in Chemical Crystallography. *Acta Crystallogr. Sect. D Biol. Crystallogr.* **2009**, *65*, 148–155.

(39) Liu, Y.; Gabriele, B.; Davey, R. J.; Cruz-Cabeza, A. J. Concerning Elusive Crystal Forms: The Case of Paracetamol. *J. Am. Chem. Soc.* **2020**, *142*, 6682–6689.

(40) Joiris, E.; Di Martino, P.; Berneron, C.; Guyot-Hermann, A. M.; Guyot, J. C. Compression Behavior of Orthorhombic Paracetamol. *Pharm. Res.* **1998**, *15*, 1122–1130.

(41) Finnie, S.; Prasad, K. V. R.; Sheen, D. B.; Sherwood, J. N. Microhardness and Dislocation Identification Studies on Paracetamol Single Crystals. *Pharm. Res.* **2001**, *18*, 674–681.

(42) Bussi, G.; Donadio, D.; Parrinello, M. Canonical Sampling through Velocity Rescaling. *J. Chem. Phys.* **2007**, *126*, 014101.

For Table of Contents Use Only

Molecular Dynamics simulation of molecular crystals under anisotropic compression: bulk and directional effects in anthracene and paracetamol

Silvia Rizzato, Angelo Gavezzotti, Leonardo Lo Presti

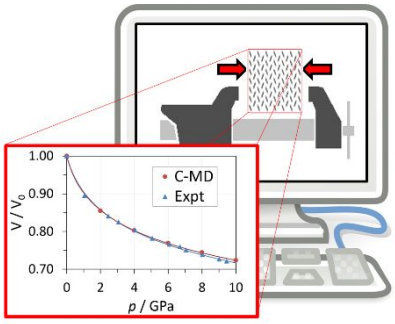

Computer simulation of molecular crystals by classical molecular dynamics under both isotropic and anisotropic external stress fields reproduces quantitatively the response of the material at high pressure, shedding light on the implied changes at the molecular–scale.

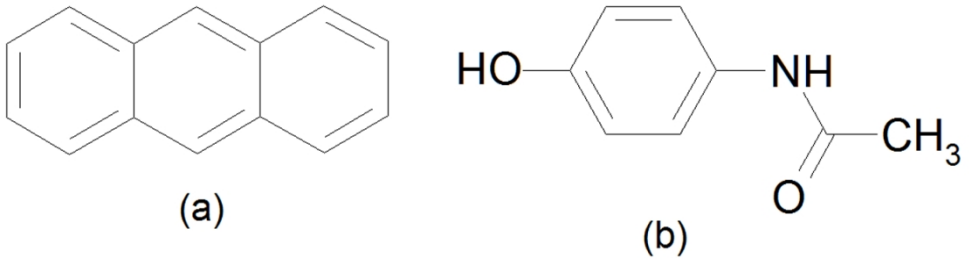

Molecular structures of anthracene (a) and N-(4-hydroxyphenyl)acetamide (paracetamol) (b).

119x33mm (300 x 300 DPI)

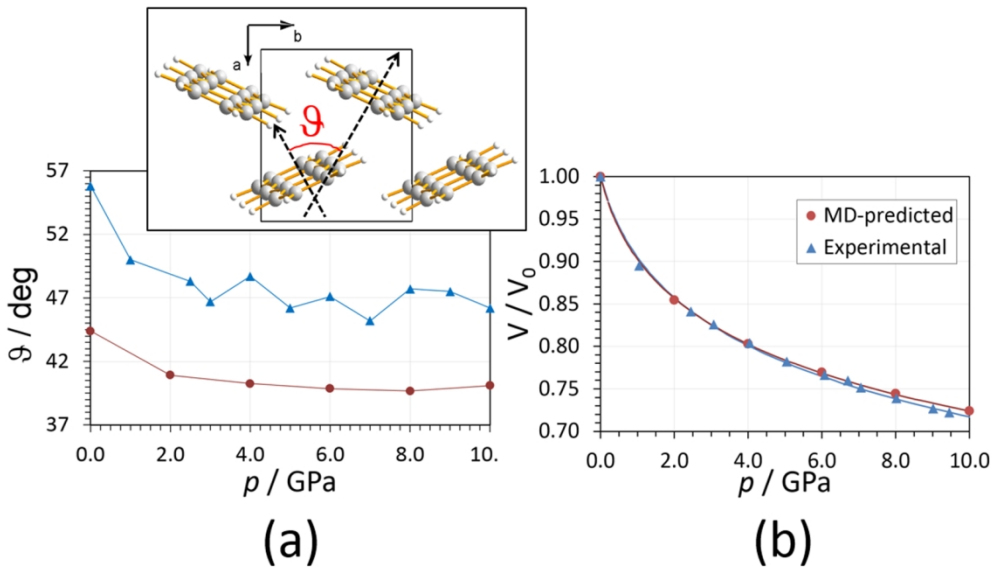

Predicted (red dots, this work) vs. experimental (blue triangles) interplanar angle θ as a function of pressure. Inset: definition of the angle θ. Lines serve only as a guide for the eye. (b) Predicted (red dots, this work) vs. experimental (blue triangles) relative change of the anthracene cell volume up to 10 GPa. V0 corresponds to ambient conditions. Lines are the least-squares fittings based on the Vinet equation of state. Individual cell edges are reported in Figure S3 SI

140x80mm (300 x 300 DPI)

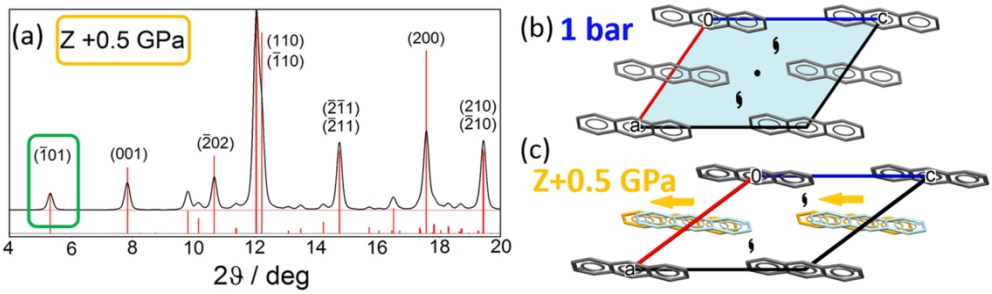

(a) Simulated powder pattern (same parameters as in Figure S7 SI) for anthracene averaged over the last 100 ps of a 200 ps–long trajectory under uniaxial compression of 0.5 GPa along the laboratory axis Z. The (1 01) reflection, symmetry–forbidden in P21/a, is highlighted in green. (b) Crystal packing of anthracene at ambient pressure in the (a,c) plane, with highlighted the a glide (cyan), the screw axes and the inversion centre. (c) Anthracene under uniaxial compression, viewed down the b axis. Molecules at ½ a corresponding to the actual C–MD prediction are coloured in yellow; cyan ones indicate where they would be if the glide a were still present. The yellow arrows highlight the slip direction.

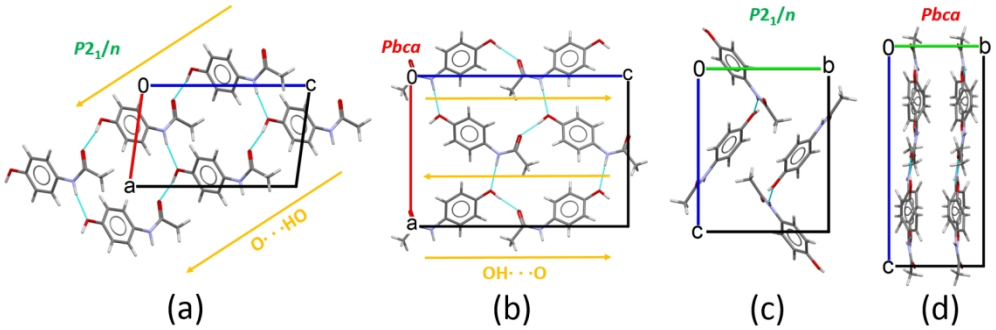

Paracetamol packing as seen down the b axis ((a) monoclinic, (b) orthorhombic) and the a axis ((c) monoclinic, (d) orthorhombic). H-bonds are drawn as cyan dotted lines. Yellow arrows highlight the direction of OH···O bonds; N-H···O links are orthogonal.

150x49mm (300 x 300 DPI)

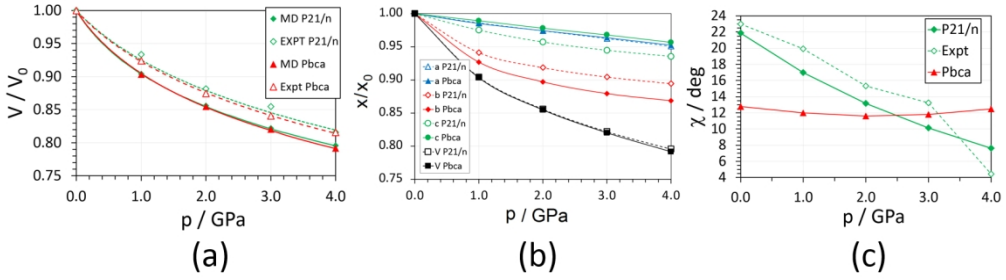

(a) Relative change of the cell volume of paracetamol, from either X-ray diffraction estimates (empty dots, dashed lines)24 and C–MD simulations (full dots, full lines). Lines are the least-squares fittings based on the Vinet equation of state.35 (b) Comparison of relative changes of lattice parameters with isotropic pressure for the P21/n (empty points) and Pbca (full points) structures, with the following colour code: blue: a; red: b; green: c; black: V. (c) Change of angle X as a function of p. Full rhombi: C–MD simulations; empty rhombi: experimental,[24] both for the P21/n structure. Red triangles: C–MD simulations, Pbca structure.

150x42mm (300 x 300 DPI)

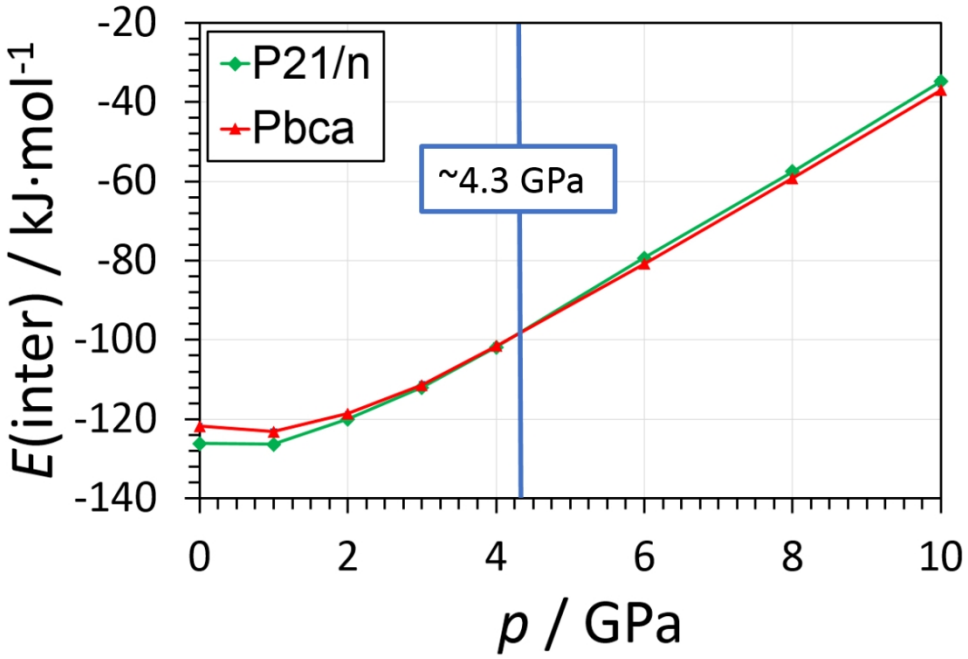

Intermolecular energy curves as a function of pressure for the two polymorphs of paracetamol. The vertical line marks the crossing point. Broken lines serve only as guides for the eye.

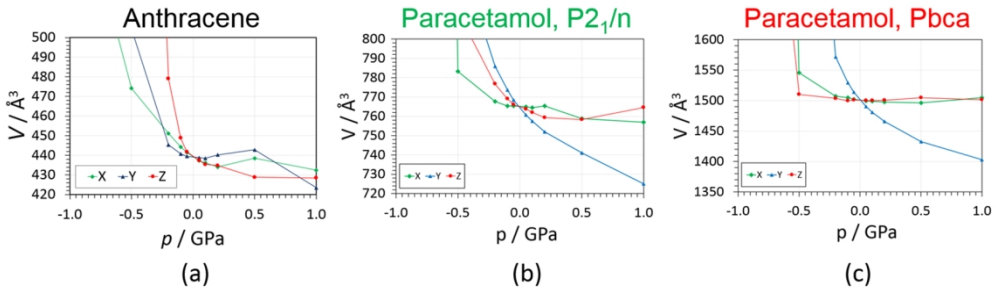

(a) Change of the cell volume due to a monoaxial stress field applied along either the X (green), Y (blue) or Z (red) laboratory axis (V, Å3) of anthracene. Negative (positive) p means tensile (compression) stress. All data points come from the average of the last 100 ps of 200 ps–long NpT trajectories. For each simulation, Sij = 0; two diagonal elements of S were set at 1.033·10−4 GPa, while the third one followed the sequence −1, −0.5, −0.2, −0.1, −0.05, +0.05, +0.1, +0.2, +0.5, +1.0 GPa. (b) and (c): Same as (a), for the two P21/n and Pbca forms of paracetamol.

150x44mm (300 x 300 DPI)